



Full length article

Using irradiation effect to study the disparate anchoring stabilities of polar-organic molecules adsorbed on bulk and thin-film metal surfaces



Kowsalya Arumugam^a, Hong-Ming Chen^a, Jing-Huan Dai^a, Mau-Fu Gao^a, Abhishake Goyal^a, Meng-Kai Lin^a, Yasuo Nakayama^b, Tun-Wen Pi^c, Sebastian Metz^{d,e}, Theodoros A. Papadopoulos^f, Horng-Tay Jeng^{a,g,h}, S.-J. Tang^{a,c,g,*}

^a Department of Physics and Astronomy, National Tsing Hua University, Hsinchu 30013, Taiwan

^b Department of Pure and Applied Chemistry, Tokyo University of Science, 2641 Yamazaki, Noda, Chiba 278-8510, Japan

^c National Synchrotron Radiation Research Center (NSRRC), Hsinchu 30076, Taiwan

^d Scientific Computing Department, STFC Daresbury Laboratory, Daresbury, Warrington WA4 4AD, UK

^e Fraunhofer Institute for Solar Energy Systems ISE, Heidenhofstraße 2, 79110 Freiburg, Germany

^f Department of Natural Sciences, Thornton Science Park, University of Chester, Chester CH2 4NU, UK

^g Institute of Physics, Academia Sinica, Taipei 11529, Taiwan

^h Physics Division, National Center for Theoretical Sciences, Hsinchu 30013, Taiwan

ARTICLE INFO

Keywords:

Irradiation effect

Chloroaluminum phthalocyanine

Photoelectron spectroscopy

Adsorption

Stability

ABSTRACT

The behavior of polar metal organic molecules, chloroaluminum phthalocyanine (ClAlPc), upon ultraviolet (UV) irradiation was investigated to evaluate the stability of the adsorption process on the Ag(111) thin film and bulk crystal. Photoelectron spectroscopy (PES) was mainly employed to measure the molecular energy states (MES) and vacuum level (VL) shift for 1-ML ClAlPc in the Cl-down configuration. A consistent trend was observed showing that ClAlPc in the Cl-down configuration is energetically more stable on the Ag thin-film surface than on the corresponding surface of the Ag bulk crystal. The intermediate adsorption state in tilted configuration during the irradiation impinging is identified by large positive VL shifts and broad spectra line shapes to infer a flipping mechanism from Cl-down to Cl-up configuration. Strain on the Ag thin films from the underlying lattice-mismatched Ge(111) substrate is considered to cause enlarged hollow sites on the Ag(111) thin-films, that anchor the Cl-down configuration more tightly on the thin-film surfaces, as confirmed by density functional theory (DFT) calculations.

1. Introduction

Organic materials have been adopted extensively in the past two decades in electronic and optoelectronic applications such as organic light emitting diodes (OLEDs), organic field effect transistors (OFETs), organic solar cells, and organic photovoltaic (OPV) devices. Developing and improving molecular devices using a broad variety of organic molecules [1–7] thus has become an area of research that sparked tremendous interest in the academic and industrial community. Generally, Metal-Phthalocyanine's (MPcs) are important for organic electronics because of their remarkable stability and specific ligand functionality towards metal electrodes. Chloroaluminium Phthalocyanine (ClAlPc), as one of polar MPcs, has received much attention due to its applications in electronic devices [8,9], especially as its two different adsorption configurations, Cl-up and Cl-down (see Fig. 1), allow the

tuning of the energy level alignment (ELA) that is crucial for charge-transport performance [10]. Manipulation of the dipole-up and dipole-down configurations of polar MPcs has shown to be possible by choosing different growing conditions or experimental techniques [11–13]. Lin et al. [13] successfully correlated the MES obtained by PES to the density of states (DOS) for the Cl-up and Cl-down configurations of ClAlPc. It was also demonstrated that the dipole orientation of the first ClAlPc layer can be controlled by adjusting the deposition rate and post annealing conditions with the ELA of the two adsorption modes of ClAlPc differing by ~ 0.4 eV.

With an Al–Cl unit generating a permanent dipole moment of 3.7 Debye for an isolated ClAlPc molecule in gas phase [14], the two different adsorption modes, i.e. Cl-up and Cl-down, of ClAlPc lead to distinct surface properties related to specific adsorption modes. For example, the VL shifts with respect to the Ag(111) work function are

* Corresponding author at: Department of Physics and Astronomy, National Tsing Hua University, Hsinchu 30013, Taiwan.

E-mail addresses: t.papadopoulos@chester.ac.uk (T.A. Papadopoulos), jeng@phys.nthu.edu.tw (H.-T. Jeng), sjtang@phys.nthu.edu.tw (S.-J. Tang).

<https://doi.org/10.1016/j.apsusc.2019.07.070>

Received 23 April 2019; Received in revised form 1 July 2019; Accepted 10 July 2019

Available online 11 July 2019

0169-4332/ © 2019 Elsevier B.V. All rights reserved.

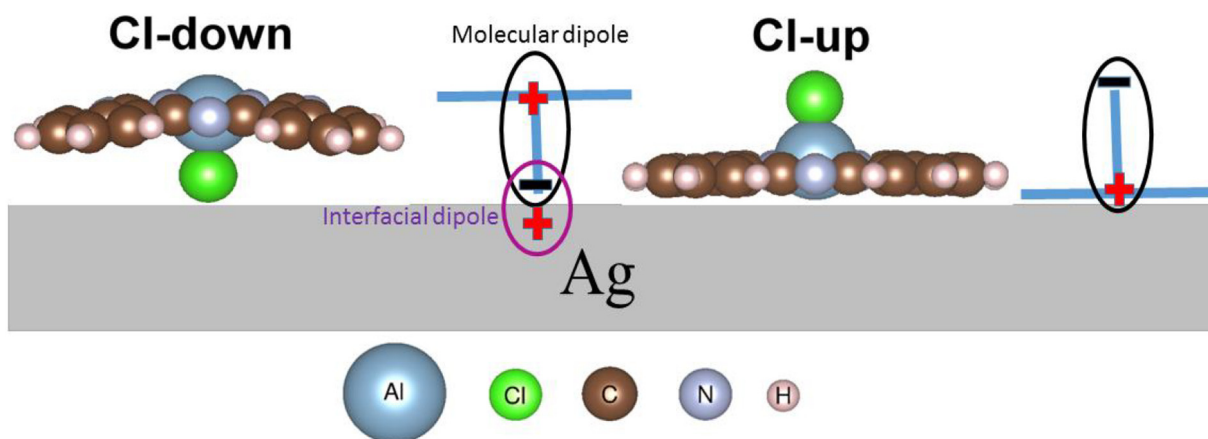


Fig. 1. The schematic illustration of ClAlPc molecules adsorbed on a Ag surface in Cl-down and Cl-up configurations with two types of dipole formation indicated.

significantly different (Fig. 2(a) of Ref. [13]). As illustrated in Fig. 1, for the Cl-down configuration, the VL shift is influenced by the Al–Cl molecular dipole as well as the Cl–Ag interfacial dipole that in view of the large differences in electronegativity [15,16] between Cl (3.16) and Ag (1.93) is expected to be strong. For the Cl-up configuration, the VL shift is mainly influenced by the Al–Cl molecular dipole and the push-back effect [13] originating from the large interaction area of the phthalocyanine (Pc) plane and the Ag(111) surface [11,17]. Another important aspect for both configurations is the adsorption stability. According to DFT calculations [13], ClAlPc has an adsorption energy of -3.56 eV in Cl-down configuration and of -5.22 eV in Cl-up configuration. While the latter can be attributed to the stabilizing interaction of the Pc molecule with the substrates surface, it is still possible to form a monolayer (ML) mainly consisting of Cl-down configuration on Ag (111) via a very slow deposition rate [13]. Hollow sites among Ag(111) atoms were considered important for the formation of the metastable Cl-down ClAlPc layer [13]. Therefore, it is physically interesting to investigate how the Cl-down configuration responds to any change of the substrate properties and intended perturbations. In this paper we employ two approaches: first, by using either a Ag film of different thickness or a Ag bulk crystal as the substrate and second, by using UV radiation light as the perturbation source. Due to the lattice mismatch with the substrate of Ge(111), there are strain effects to be expected within the Ag thin film [18,19]. In this case, the increased Ag–Ag distance of the surface atoms imposes a larger hollow site, which in turn allows the Cl atom of the Cl-down configuration to anchor deeper, providing further energetic stabilization. In contrast, on the Ag(111) bulk surface, the Cl-down configuration is expected to have disparate energetic stability. The energy and pressure inflicted by irradiation impinging to the ClAlPc molecule can further probe the adsorption stability. We have measured and analyzed the dependence of photoemission line shapes of the MES and VL shifts of 1-ML Cl-down ClAlPc on photon flux and exposure time. We indeed found that the Cl-down configuration of ClAlPc is more stable on the Ag thin-film than on the Ag bulk crystal surface. The explanation for this finding seems to be related to the Ag bond strain imposed by Ge(111) and is provided with the assistance of DFT calculations. In addition, the crossover mechanism from the Cl-down to the Cl-up configuration is proposed upon irradiation impinging.

2. Experimental procedures and methods

A N-type Ge(111) wafer and a bulk Ag(111) crystal were chosen as starting substrates for ClAlPc. The clean substrates were achieved by standard sputtering and annealing procedure and confirmed by sharp low-energy electron diffraction (LEED) unveiling the Ge(111)-c(2×8) and the Ag(111)- 1×1 patterns. Ag films of 7, 9 and 16 ML were

deposited onto the clean Ge(111) substrate at around -130 °C to -140 °C, followed by annealing at ~ 35 °C to attain the uniform films [13,20]. The thickness of Ag films was determined by the calibrated thickness-dependent energy positions of Ag quantum-well states (QWS) [13,20]. ClAlPc molecules were thermally deposited onto surfaces of Ag films and the bulk Ag(111) at room temperature. The deposition rate was determined by the precalibrated quartz thickness monitor. We found that for forming 1-ML ClAlPc in Cl-down configuration on Ag films and the bulk Ag(111), the optimal deposition rates are 0.1 and 0.04 Å/min, respectively. 1-ML ClAlPc was determined by the coverage-dependent VL shift and further calibrated by the photoemission intensity ratio between ClAlPc MES and Ag substrate states [13]. PES experiments were carried out with 50-eV photons and the photon fluxes were controlled by the slit and measured by the mesh currents at the 08A1-LSGM beamline of the National Synchrotron Radiation Research Center (NSRRC), Hsinchu, Taiwan. Based on the previously calibrated relation between the photon flux and the mesh currents, the photon-flux values were determined. The energy resolution of the PES system is 50 meV and the spectra was taken along the $\bar{\Gamma}\bar{M}$ symmetry direction of the Ag(111) surface Brillouin zone. To obtain the VL shift, the sample was electrically biased -6.0 V at normal emission [13] in order to shift the secondary cutoff into an energy range suitable for detection by the electron analyzer.

The ab-initio calculations were performed using the Vienna Ab-initio Simulation Package (VASP) [21–23] based on density functional theory (DFT). The Perdew–Burke–Ernzerhof (PBE) [24] generalized-gradient-approximation functional, and the projector augmented wave (PAW) [25,26] method are employed in the self-consistent calculations. The ClAlPc/Ag(111) system is simulated by putting a ClAlPc molecule on top of the Ag(111) 6×6 supercell with the thickness of 3 Ag layers. The Ag(111) 6×6 supercell adopted here is approximately the smallest one that can accommodate the ClAlPc molecule without imposing steric effects. By adjusting the lattice constant of the Ag substrate from 4.09 to 4.40 Å, we study the evolution of the energy change of ClAlPc with both the Cl-down and the reversed Cl-up orientation. For each case, we fixed the lattice constant while the atomic positions were optimized until the total energy converges within 10^{-4} eV. The plane-wave cutoff energy is set at 400 eV on $6 \times 6 \times 1$ k-mesh over the 2D Brillouin zone.

3. Results and discussion

The photoemission spectra in Fig. 2(a)–(c) shows a series of energy distribution curves (EDCs) for a step-by-step incremental deposition of ClAlPc onto Ag films of 7 and 9 ML deposited on Ge(111), and a single bulk Ag(111) crystal surface. For ClAlPc on Ag films, a single peak located at -9.70 eV emerges and increases in intensity up to 1 ML ClAlPc. As was demonstrated in a previous study [13], this peak

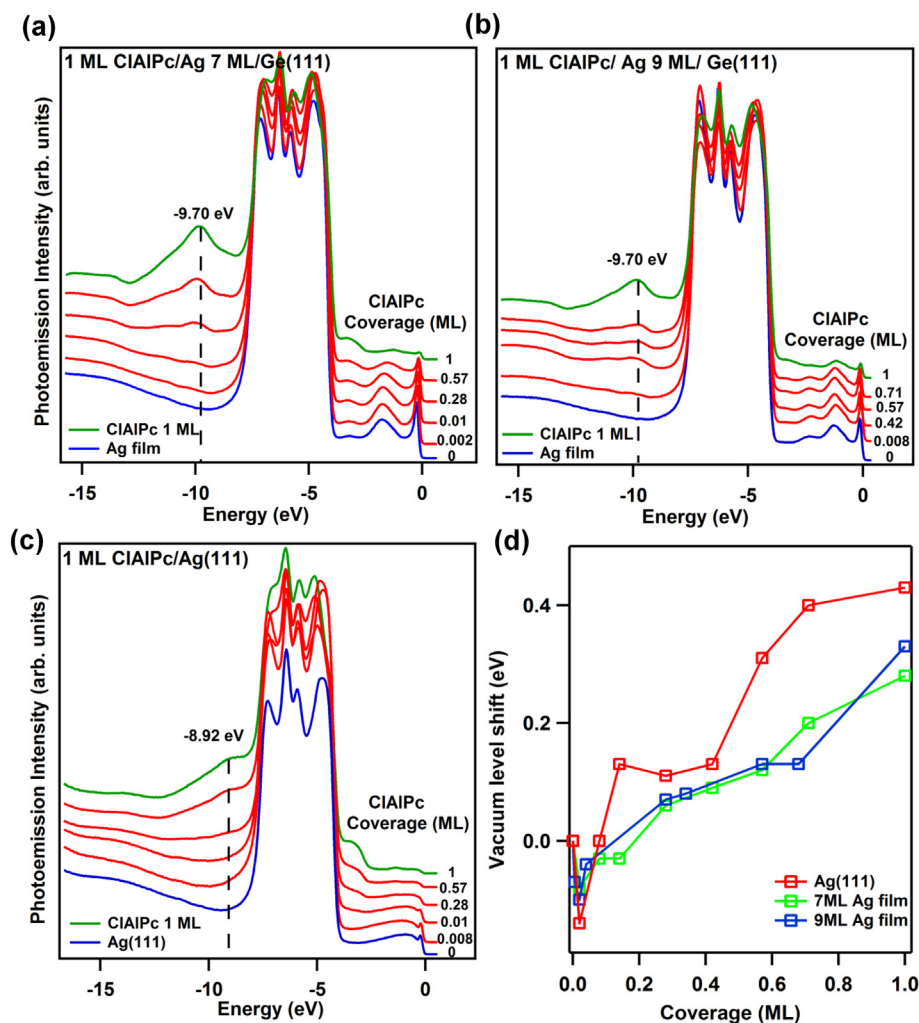


Fig. 2. Coverage dependent photoemission spectra of CIAIPc on (a) a 7-ML Ag film, (b) a 9-ML Ag film (c), and a Ag(111) bulk crystal surface. (d) VL shift as a function of CIAIPc coverage on a 7-ML Ag film, a 9-ML Ag film, and a Ag(111) bulk crystal surface. Blue and green colors of EDCs denote the CIAIPc at the coverage of 0 and 1 ML (3.5 Å).

(previously measured at -9.71 eV) represents the MES of the Cl-down configuration. The peak for CIAIPc on a bulk Ag crystal surface turns out to be different; the emerging peak is a lot broader and the energy position of -8.92 eV is closer to that for a Cl-up configuration (previously measured at -8.76 eV) [13]. The broadness of the peak and the shifted energy, however, indicates that the peak might result from more than a single molecular configuration.

Fig. 2(d) shows the corresponding coverage dependence of the VL shifts for the cases in Fig. 2(a)–(c). As can be seen, the VL shifts for CIAIPc deposited on the bulk Ag crystal are larger than those on Ag films. This is in contrast to the previous observation that VL shifts for Cl-up configuration are lower than those for Cl-down configuration (Fig. 2(a) of Ref. 13). This finding points towards the presence of an intermediate configuration between Cl-up and Cl-down. The only configuration that fulfills the observed VL shift requirements is a tilted configuration, with a surface interaction between that of Cl-down and Cl-up.

The deposition rates for CIAIPc on Ag films and the bulk Ag(111) crystal surface are relatively low and very similar in all cases so they are unlikely to be the cause of the observed differences in spectra. Due to the fact that the collected coverage-dependent photoemission data set in Fig. 2(a)–(c) undergo elongated exposure for hours to the irradiation, the adsorption configurations of organic molecules, especially those in a metastable state, could alter over exposure time. In other words, the

stability of the absorbed molecules can be examined by the irradiation effect. Fig. 3(a) and (b) shows a series of time-dependent photoemission spectra of 1 ML CIAIPc in Cl-down configuration deposited on 7-ML Ag thin film and a Ag bulk crystal surface, respectively under radiation exposure with a flux of 3.15×10^{13} photons/s. The evolution of the peak line shape within the energy range of -10 eV to -9.8 eV is evident; for both cases, the peaks decay in intensities and shift towards higher energies. The final curves after 50 min of radiation exposure (black) were fitted using two Lorentzians representing the Cl-up (green, centered at -8.6 eV) and the Cl-down (amber, centered at -9.7 eV) configuration, and a smooth polynomial background (grey). As seen, for CIAIPc on 7-ML Ag film, the peak line shape still shows Cl-down component (amber) dominates but for CIAIPc on bulk Ag(111) crystal surface, the Cl-up component (green) has the same intensity as that of the Cl-down component. This explains the results of Fig. 2; after prolonged radiation exposure, CIAIPc stays mainly at Cl-down configuration on Ag thin films, but partially evolves to Cl-up configuration on bulk Ag(111) crystal. Fig. 3(c) shows a series of time-dependent photoemission spectra of 1 ML CIAIPc on bulk Ag(111) crystal with the reduced photon flux of 2.11×10^{13} photons/s. The fitting to the peak of the last EDC still exhibits the equal composition of both configurations, namely, the same intensity of the two fitting Lorentzians, but the line widths are obviously narrower than those in Fig. 3(a). This implies that more CIAIPc molecules in the intermediate state between Cl-down and Cl-up

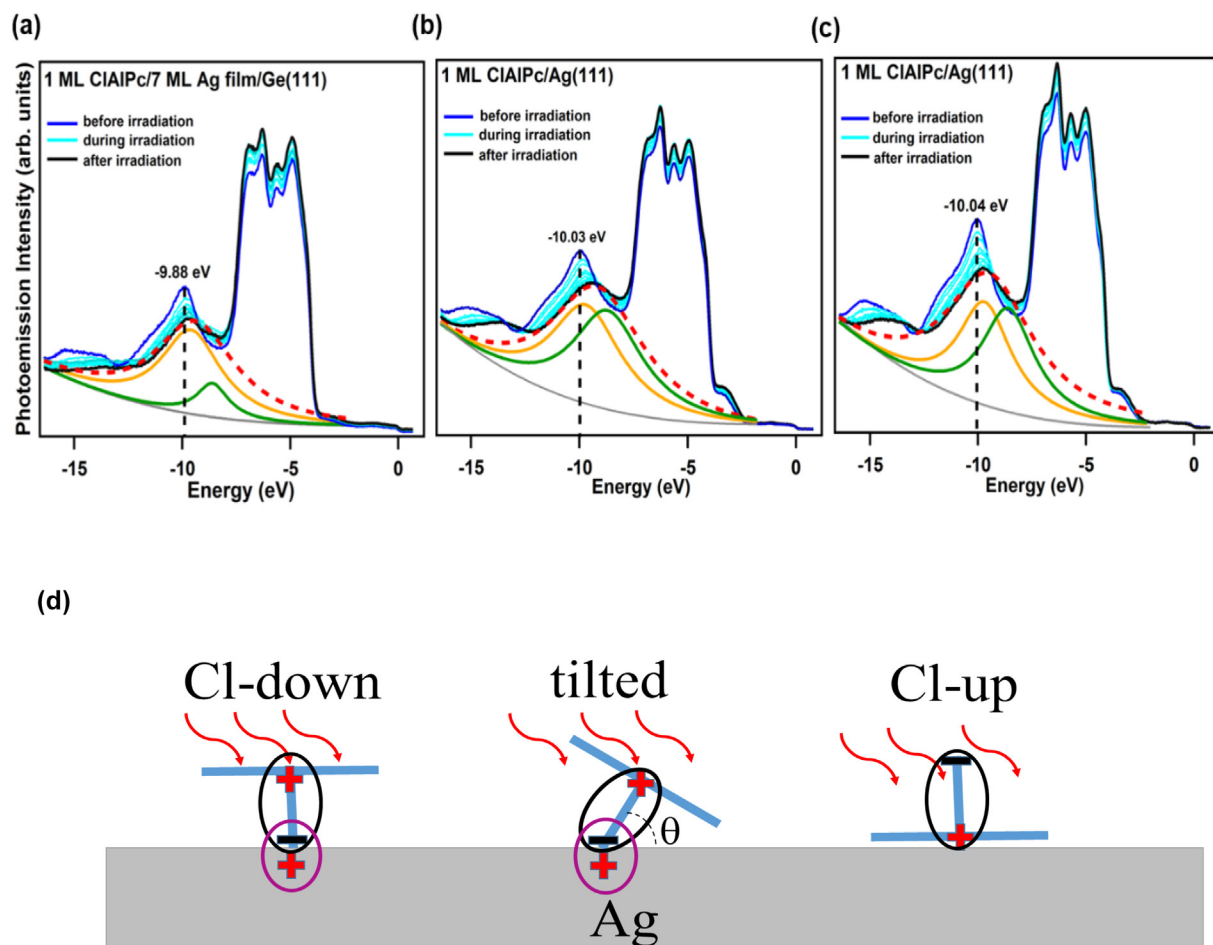


Fig. 3. Time-dependent photoemission spectra of 1 ML ClAlPc on (a) a 7-ML Ag film and (b) a Ag(111) bulk crystal surface undergoing irradiation impinging at the photon fluxes of 3.15×10^{13} photons/s. (c) The same as (b) but with the photon fluxes of 2.11×10^{13} photons/s. The amber and green curves indicate the fitting components of Cl-down and Cl-up configurations. The grey curve indicates the fitting background. The red dashed curve indicates the total fitting result. The energy positions of the Cl-down peak before irradiation impinging are marked with the vertical dashed lines. (d) The schematic model to illustrate the flipping process from Cl-down to Cl-up configuration under irradiation impinging.

are produced under more-intense radiation exposure since the tilted configuration can be regarded as the incomplete one of either the Cl-up or Cl-down; the corresponding MES peaks shift away from the original positions of both configurations to cause the broadening. The measured VL shifts upon radiation exposure for the three cases in Fig. 3(a)–(c) are 0.28, 0.37, and 0.48 eV, respectively. As shown in Fig. 1, the contributions to the positive VL shift of the Cl-down configuration originate from the Cl–Ag interfacial dipole. For the Cl-up configuration, the push-back effect dominates the negative VL shift of the Cl-up configuration. The question remains, however, why the measured VL shifts are positive and large for all the cases of Fig. 3(a)–(c), where parts of Cl-down ClAlPc molecules were driven to the Cl-up configuration by irradiation impinging? We believe there is an intermediate state of tilted configuration for Cl-down ClAlPc to flip to Cl-up one during the irradiation impinging, as depicted in Fig. 3(d). Scanning tunneling microscopy (STM) [27–30] indicated that the tunneling of the Cl atom through the Pc plane is the most energy-efficient way for the switching between the Cl-down and the Cl-up configuration. But, in our case, the impinging photons don't just carry energy but also impose radiation pressure into the molecules, so the anchoring point for a Cl atom on Ag surface may work as a rotational pivot for the flipping. The radiation pressure derived from the photon fluxes employed in Fig. 3(b) and (c) are 8.42×10^{-13} and 5.64×10^{-13} N/m², respectively. When the Cl-down ClAlPc is tilted, the VL would increase based on two possible reasons: First, the vertical component of the molecular dipole length

decreases due to the tilted angle θ as shown in Fig. 3(d) so the negative contribution to the VL shift from the Al–Cl molecular dipole moment would be correspondingly reduced, and the total VL shift, which is the sum of negative contribution from molecular dipole and positive contribution from interfacial dipole (illustrated in Fig. 1), would increase. Second, due to the irradiation impinging, the molecular dipole would be deformed so that the Cl–Al bond becomes weaker, leading to even more charge transfer to Cl atom from Ag to cause larger positive VL shift than the case of Cl-down configuration.

To further confirm this picture, we investigate the irradiation effect on 1-ML ClAlPc/Ag(111) bulk crystal for the two following cases: Cl-down and Cl-up configurations coexisting (see Fig. 4(a)) and Cl-down configuration dominating (see Fig. 4(b)). For the first case, the EDC line shape in the beginning exhibits two distinct peaks; one for Cl-down at -10.48 eV and one for Cl-up at -9.05 eV. Note that the different energy positions of these peaks from those of single Cl-down and Cl-up peaks, -9.7 eV and -8.6 eV, are due to the change of ELA. As shown in the sketch of coexisting configurations for ClAlPc at the top of Fig. 4(a), Cl-down and Cl-up ClAlPc should anchor side by side to ensure stability by the attraction force between opposite dipole moments [31]. With this type of arrangement, Cl-down ClAlPc is less likely tilted or even flipped upon irradiation impinging than the second case of Cl-down dominating configuration. However, after 50-min radiation impinging, the peak shape shows almost a complete Cl-up peak for the first case as shown in the middle part of Fig. 4(a), inferring mainly the tunneling

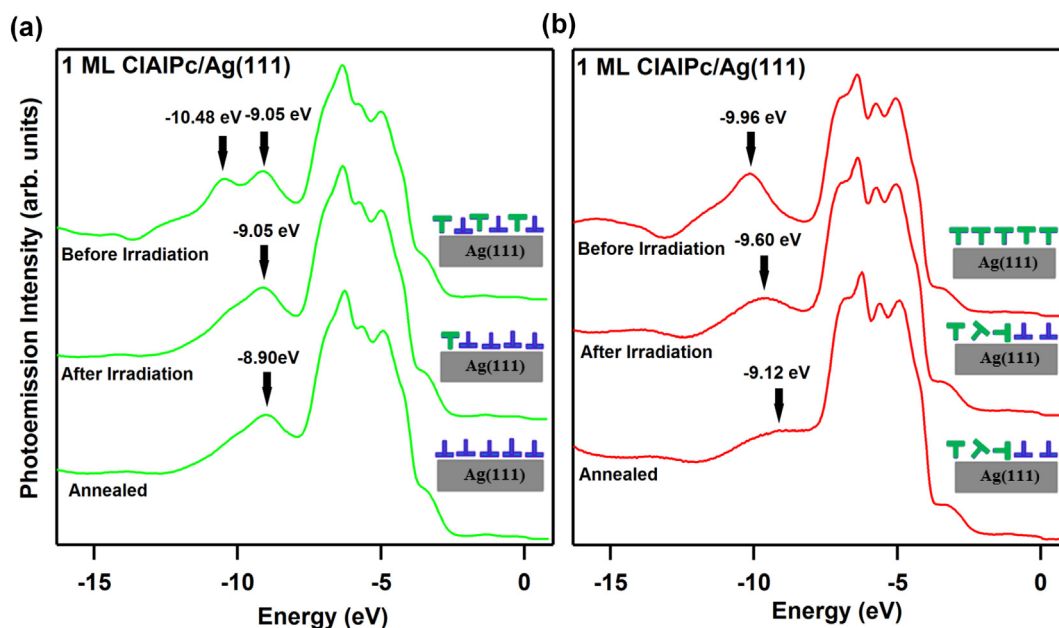


Fig. 4. Photoemission spectra of 1-ML ClAlPc on Ag(111) bulk crystal before and after irradiation, and after subsequent annealing for (a) coexisting Cl-down and Cl-up configurations and (b) dominant Cl-down configuration. The arrows indicate the energy positions of peak maximums.

mechanism to switch from Cl-down to Cl-up configuration. The middle part of Fig. 4(b), the second case, shows the EDC for 1-ML Cl-down ClAlPc on bulk Ag(111) crystal after 50-min radiation impinging. The peak line shape is a lot broader, manifesting disordered tilted configuration. The measured VL shifts after 50 min radiation impinging in the first and second cases are 0.14 and 0.37 eV. The much larger positive increase of VL shift for the latter case is in line with the picture depicted in Fig. 3(d). In both cases, annealing at 60 °C for 30 min was carried out after irradiation. As seen from the bottoms of Fig. 4(a) and (b), Cl-up peak is shaper with VL shift of -0.1 eV in the first case, but the broad peak in the second case become even broader with VL shift of 0.05 eV, indicating a more complete Cl-up configuration and the robustness of the tilted configuration, respectively.

Since Cl-down configuration is more stable on Ag thin films than on the bulk Ag(111) crystal, it is very interesting to further investigate the stability dependence on the thickness of Ag thin films. Fig. 5(a) shows the EDCs taken at normal emission for a clean bulk Ag(111) crystal surface, and 7-, 9-, and 16-ML Ag films grown on Ge(111). For the bulk Ag(111) crystal surface, the main features are a sharp Shockley surface state (SS) about -0.1 eV and a broad bulk edge near -0.3 eV [32]. For Ag thin films, in addition to the surface states, a series of QWS peaks marked with different quantum numbers v 's in the EDCs characterize the Ag thickness with their energy positions [20,33,34]. The comparison between EDCs before (dashed curves) and after (solid curves) 50-min irradiation impinging with the flux of 3.15×10^{13} photons/s for 1-ML Cl-down ClAlPc on the bulk Ag(111) crystal and Ag thin films are presented respectively in Fig. 5(b). It is noteworthy that the initial energy positions for the Cl-down peaks are different, as marked in Fig. 5(b), as the initial anchoring is not settled. After irradiation impinging, the Cl-down peaks of all the cases shift to the positions near -9.7 eV as indicated by the vertical dashed line, but the line widths become broader for the bulk Ag(111) crystal and 16-ML Ag film than the 7- and 9-ML Ag films. The enhancement of the shoulder at about -3.8 eV for the former, mainly representing the partial DOS from Cl for Cl-up configurations [13], also indicate that some Cl-down ClAlPc molecules flipped to a Cl-up configuration. We further fitted the peak line shapes during irradiation impinging with two Lorentzians representing Cl-down and Cl-up components and plot the intensities of the two components versus exposure time in Fig. 5(c) and (d). The time dependence of the peak component intensities was approximated by

$I = \pm I_0 e^{-t/\tau} + c$, where τ is the time constant and c is an offset constant. Positive and negative signs of the exponential function are for the decrease of the Cl-down and increase of Cl-up components, respectively. For the decay of the Cl-down peak, the extracted time constants are, $\tau = 27.7, 17.7, 16.69,$ and 11.14 mins for ClAlPc on 7- and 9-ML, 16-ML Ag films and bulk Ag(111) crystal surfaces, and for the growing of Cl-up peaks are 23.25, 12.98, 11.76, and 10.92 mins. Therefore, the higher stability of the Cl-down configuration on thinner Ag films is evidently indicated by the larger time constant for both the Cl-down and the Cl-up configurations. In addition, the rougher surface of 16-ML Ag film/Ge(111) as indicated by the low and broadened SS and QWS in Fig. 5(a) has closer adsorption stability to the uniform bulk Ag(111) surface, ruling out the surface defect or roughness as the effective factor for the adsorption stability.

Fig. 6(a) and (b) show the LEED patterns of a clean Ag(111) bulk crystal surface and a 7-ML Ag thin film, respectively. The lattice mismatch between Ag(111) and Ge(111) is 28% in terms of their bulk lattices ($a_{\text{Ag}} = 4.08 \text{ \AA}$, $a_{\text{Ge}} = 5.66 \text{ \AA}$) when their symmetry axes are aligned with each other. Therefore, the Ag thin films growing parallel to Ge(111) would be subject to tensile strain effects that enlarge the sizes of the hollow sites between Ag atoms, which have been observed to be the anchoring positions for Cl-down ClAlPc molecules on Cu(111) [35]. As observed, the LEED spots of the Ag film with arc shapes are indeed much broader than those of the bulk Ag(111) crystal surface but the spot positions are about similar, indicating that the actual tensile strain exerted on the Ag films is a lot smaller than 28%. The arc lengths indicate a mosaic structure of films rotating over a certain range and this was considered as a spontaneous mechanism for reducing large lattice mismatch [36,37]. It is noteworthy that the same LEED-spot shape was also observed from a strained Ag film on the lattice-mismatched Si(111) substrate, and the strain effect was used to explain the depopulation of the SS of the Ag film [19]. In that case, the lattice mismatch in terms of the bulk lattices was 25% and the tensile strain of 0.95% was estimated to make the occupied Ag-film surface state shift 0.15 eV to the energy position above Fermi level [19]. The SS of Ag films on Ge(111) is however more robust to the strain because it has strong hybridization coupling with the Ge band edges [38]. We carried out the DFT calculations for the Cl-up and Cl-down configurations on Ag slabs with varied lattice constants ranging from 4.09 Å, near the bulk counterpart, to 4.40 Å. Fig. 7(a)–(c) shows the top and the side views of the model

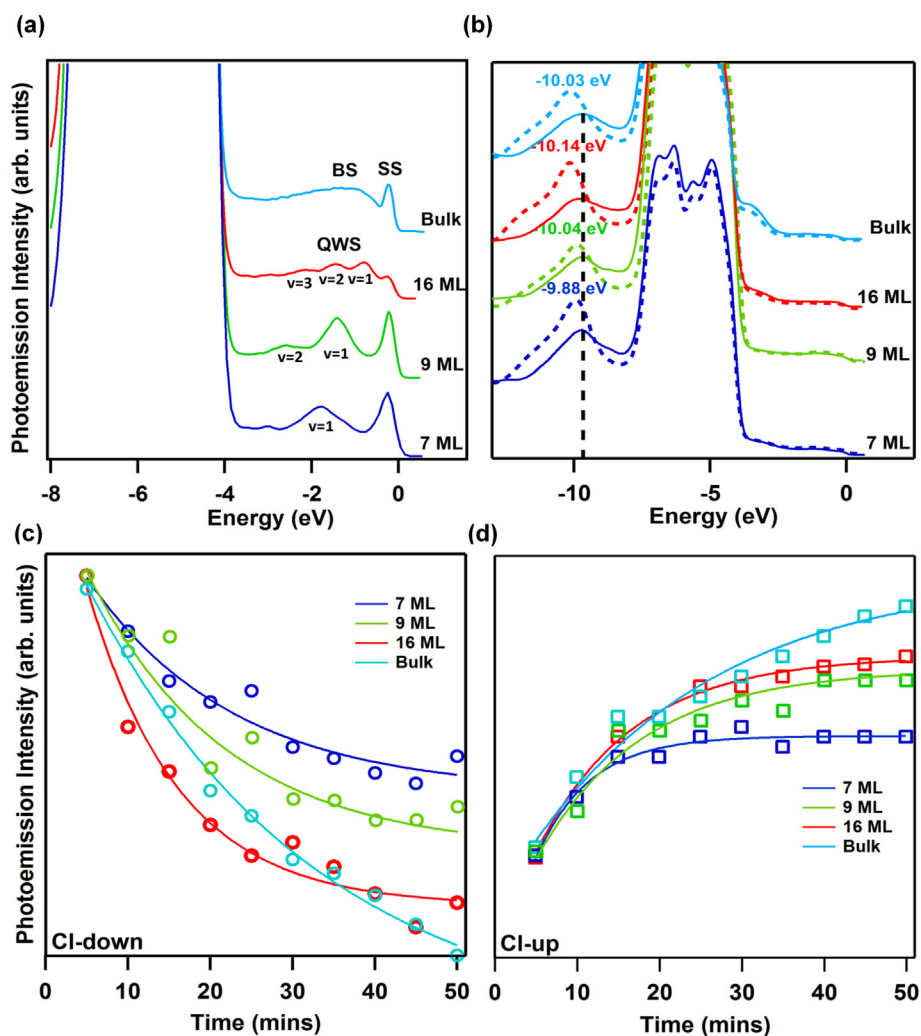


Fig. 5. Photoemission spectra of EDCs for (a) 7-, 9-, 16- ML Ag films on Ge(111), and the Ag(111) bulk crystal surface, and (b) 1-ML Cl-down ClAlPc before (dashed curves) and after (solid curves) radiation impinging on 7-, 9-, 16-ML Ag films and the Ag(111) bulk crystal. The vertical dashed line indicates the energy position of -9.7 eV. (c) & (d) Intensity as a function of radiation exposure time for Cl-down and Cl-up components.

layouts for the calculation. The resulting total energies for Cl-up and Cl-down configurations are exhibited in Fig. 7(d): The key results to be taken from this graph is that upon lattice increase from Ag bulk lattice, the energy of the system increases slower for the Cl-down than for the Cl-up configuration, with a crossover of the two configurations being

observed at about 4.3 \AA . To isolate the effect of the relative orientation, we subtract the total energy of Cl-up from that of Cl-down configuration as shown in Fig. 7(e) (as the difference between the total energies of both configurations approximately cancels out the contribution from the Ag slabs). The overall descending behavior with the increasing Ag

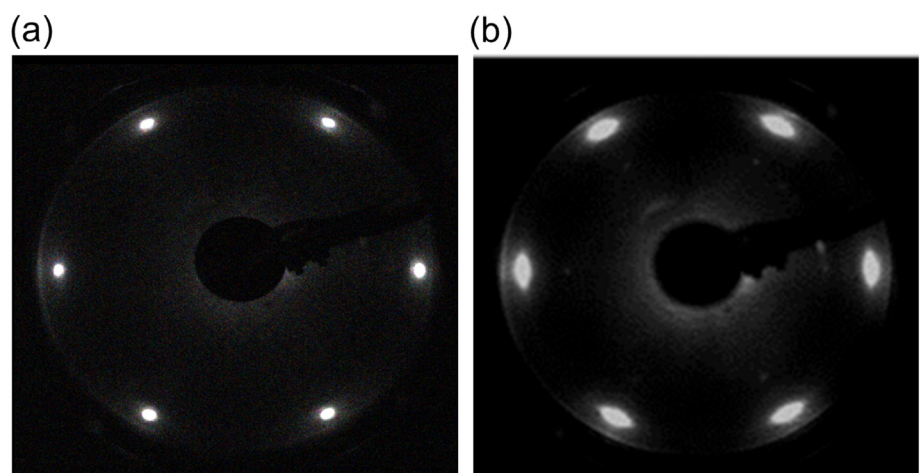


Fig. 6. LEED patterns of (a) a Ag(111) bulk crystal surface and (b) a 7-ML Ag thin film on Ge(111), taken at the electron energy 50 eV.

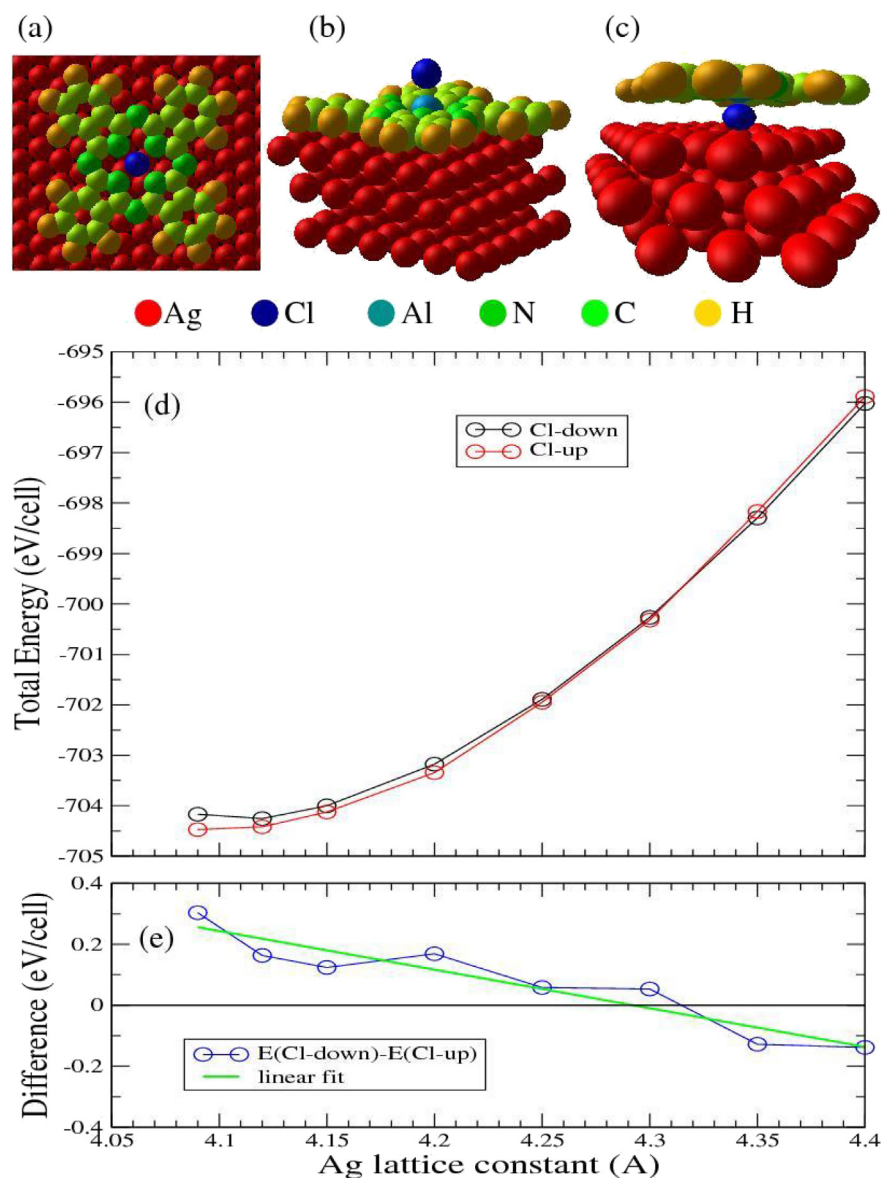


Fig. 7. Lattice structure, total energy, and out-of-plane charge profile of ClAlPc/Ag(111). (a) Top view and (b) side view of the ClAlPc molecule on top of Ag(111) 6×6 supercell with the Cl ion heading up (Cl-up). (c) Side view of the ClAlPc molecule on top of Ag(111) 6×6 supercell with the Cl ion heading down (Cl-down). (d) Total energy of the supercell with Cl-up and Cl-down orientations as functions of Ag lattice constant from 4.09 Å (single bulk crystal) to 4.40 Å (film). (e) Difference in total energies of Cl-up and Cl-down configuration.

lattice is indicated by the fitting line with negative slope. So the take home message is that the Cl-down configuration starts more stable, right when the tensile strain on the Ag lattice increases from zero.

4. Summary

In conclusion, by analyzing the photoemission spectra line shape of MES and VL shifts, we investigated the time-dependent behavior of Cl-down ClAlPc under irradiation exposure. It was observed that it anchors more stably on Ag thin films than on the bulk Ag(111) crystal surface, and a description of how the transition from Cl-down to Cl-up configuration occurs was presented. Unlike thermal annealing, incident radiation doesn't just inflict energy but pressure to the Cl-down ClAlPc molecule so it would tend to flip with the tilted configuration at the intermediate stage as revealed from the large increase of VL and broad spectra line shape. This is different from the tunneling mechanism suggested by STM that switches between Cl-down and Cl-up configuration of the ClAlPc molecule by applying negative and positive bias voltage from the STM tip [28] with the potential application to the molecular digit memory proposed [27]. Our probing of the switching mechanism via irradiation gains deeper insight. Specially, the irradiation-impinging effect we discovered can be employed to modify the

adsorption configurations of other functional molecular dipoles for various purposes, initiating a new direction in terms of the impact of irradiation on polar organic molecules. The higher stability of Cl-down ClAlPc on Ag thin films is attributed to strain effects due to a large lattice mismatch, between the Ag thin film and underlying Ge(111) substrate. Our results are in line with DFT calculations based on a slab model of the Ag(111)/ClAlPc interface for varied lattice constants. This finding provides a new avenue that may enhance the controlled fabrication process of organic optoelectronic devices at the nanoscale. In addition, we expect our result to launch further advanced studies of relevant irradiation effects, such as photon-energy dependence, on the adsorption of polar-organic molecules.

Acknowledgments

This research was supported by the Ministry of Science and Technology of Taiwan (Grant No. MOST 105-2112-M-007-017-MY3 and MOST 106-2923-M-007-001-MY4 for S.-J.T., and Grant No. MOST 106-2112-M-007-012-MY3 for H.-T. J.) This work was also partially supported by JSPS-KAKENHI Grant Numbers JP15H05498 and JP16K14102. Preliminary computations were performed at the Science and Technology Facilities Council (STFC), Daresbury Laboratory, U.K.,

and the Edinburgh Parallel Computing Centre (EPCC), via an “Open Access to Tier-2” resource allocation grant, provided by the Engineering and Physical Sciences Research Council (EPSRC), U.K. T. P. gratefully acknowledges financial support from the Royal Society under grant number IEC\R3\183088. H.-T.J. acknowledges NCHC, CINC-NTU, iMATE-AS, and CQT-NTHU-MOE, Taiwan for technical supports and S.-J. T. thanks NSRRC staff, J.-Y. Yuh, for technical assistance.

References

- [1] S. Yogev, R. Matsubara, M. Nakamura, U. Zschieschang, H. Klauk, Y. Rosenwaks, Fermi level pinning by gap states in organic semiconductors, *Phys. Rev. Lett.* 110 (2013) 036803.
- [2] Y.-H. Chen, Y.-J. Chang, G.-R. Lee, J.-H. Chang, I.W. Wu, J.-H. Fang, S.-H. Hsu, S.-W. Liu, C.-I. Wu, T.-W. Pi, Formation of gap states and enhanced current injection efficiency in organic light emitting diodes incorporated with subphthalocyanine, *Org. Electron.* 11 (2010) 445–449.
- [3] R.A. Street, M. Schoendorf, A. Roy, J.H. Lee, Interface state recombination in organic solar cells, *Phys. Rev. B* 81 (2010) 205307.
- [4] W.L. Kalb, S. Haas, C. Krellner, T. Mathis, B. Batlogg, Trap density of states in small-molecule organic semiconductors: a quantitative comparison of thin-film transistors with single crystals, *Phys. Rev. B* 81 (2010) 155315.
- [5] V. Chauhan, R. Hatton, P. Sullivan, T. Jones, S.W. Cho, L. Piper, A. deMasi, K. Smith, Elucidating the factors that determine the open circuit voltage in discrete heterojunction organic photovoltaic cells, *J. Mater. Chem.* 20 (2010) 1173–1178.
- [6] F. Petraki, H. Peisert, I. Biswas, T. Chassé, Electronic structure of co-phthalocyanine on gold investigated by photoexcited electron spectroscopies: indication of Co ion–metal interaction, *J. Phys. Chem. C* 114 (2010) 17638–17643.
- [7] C.-H. Yuan, C.-C. Lee, C.-F. Liu, Y.-H. Lin, W.-C. Su, S.-Y. Lin, K.-T. Chen, Y.-D. Li, W.-C. Chang, Y.-Z. Li, T.-H. Su, Y.-H. Liu, S.-W. Liu, Cathodic-controlled and near-infrared organic up converter for local blood vessels mapping, *Sci. Rep.* 6 (2016) 32324.
- [8] L. Li, W. Hu, H. Fuchs, L. Chi, Controlling molecular packing for charge transport in organic thin films, *Adv. Energy Mater.* 1 (2011) 188–193.
- [9] E. Lee, C.J. Andrews, A. Anctil, An iterative approach to evaluate and guide fine chemical processes: an example from chloroaluminum phthalocyanine for photovoltaic applications, *ACS Sustain. Chem. Eng.* 6 (2018) 8230–8237.
- [10] J. Zhu, C. Wang, J. Yu, F. Yang, Y. Zheng, X. Li, B. Wei, Optical simulation and experimental determination of the effect of subcell sequence in tetraphenylidibenzoperiflanthene- and phthalocyanine-based tandem solar cells, *Phys. Status Solidi A* 214 (2017) 1700340.
- [11] Y.L. Huang, W. Chen, F. Bussolotti, T.C. Niu, A.T.S. Wee, N. Ueno, S. Kera, Impact of molecule-dipole orientation on energy level alignment at the submolecular scale, *Phys. Rev. B* 87 (2013) 085205.
- [12] M. Polek, F. Latteyer, T.V. Basova, F. Petraki, U. Aygül, J. Uihlein, P. Nagel, M. Merz, S. Schuppler, T. Chassé, H. Peisert, Chemical reaction of polar phthalocyanines on silver: chloroaluminum phthalocyanine and fluoroaluminum phthalocyanine, *J. Phys. Chem. C* 120 (2016) 24715–24723.
- [13] M.-K. Lin, Y. Nakayama, Y.-J. Zhuang, K.-J. Su, C.-Y. Wang, T.-W. Pi, S. Metz, T.A. Papadopoulos, T.C. Chiang, H. Ishii, S.J. Tang, Control of the dipole layer of polar organic molecules adsorbed on metal surfaces via different charge-transfer channels, *Phys. Rev. B* 95 (2017) 085425.
- [14] H. Fukagawa, S. Hosoumi, H. Yamane, S. Kera, N. Ueno, Dielectric properties of polar-phthalocyanine monolayer systems with repulsive dipole interaction, *Phys. Rev. B* 83 (2011) 085304.
- [15] J.X. Tang, C.S. Lee, S.T. Lee, Electronic structures of organic/organic heterojunctions: from vacuum level alignment to Fermi level pinning, *J. Appl. Phys.* 101 (2007) 064504.
- [16] H. Song, N. Li, H. Zhu, Z. Peng, W. Zhao, H. Chen, W. Chen, Y. Wang, K. Wu, Dipole and charge effects of chloroaluminum phthalocyanine revealed by local work function measurements at sub-molecular level, *Chin. Chem. Lett.* 29 (2018) 429–432.
- [17] P.C. Rusu, G. Giovannetti, C. Weijtens, R. Coehoorn, G. Brocks, First-principles study of the dipole layer formation at metal-organic interfaces, *Phys. Rev. B* 81 (2010) 125403.
- [18] S.J. Tang, L. Basile, T. Miller, T.C. Chiang, Breakup of quasiparticles in thin-film quantum wells, *Phys. Rev. Lett.* 93 (2004) 216804.
- [19] G. Neuhold, K. Horn, Depopulation of the Ag(111) surface state assigned to strain in epitaxial films, *Phys. Rev. Lett.* 78 (1997) 1327–1330.
- [20] S.J. Tang, W.-K. Chang, Y.-M. Chiu, H.-Y. Chen, C.-M. Cheng, K.-D. Tsuei, T. Miller, T.C. Chiang, Enhancement of subband effective mass in Ag/Ge(111) thin film quantum wells, *Phys. Rev. B* 78 (2008) 245407.
- [21] G. Kresse, J. Hafner, Ab initio molecular dynamics for open-shell transition metals, *Phys. Rev. B* 48 (1993) 13115–13118.
- [22] G. Kresse, J. Furthmüller, Efficient iterative schemes for ab initio total-energy calculations using a plane-wave basis set, *Phys. Rev. B* 54 (1996) 11169–11186.
- [23] G. Kresse, J. Furthmüller, Efficiency of ab-initio total energy calculations for metals and semiconductors using a plane-wave basis set, *Comput. Mater. Sci.* 6 (1996) 15–50.
- [24] J.P. Perdew, K. Burke, M. Ernzerhof, Generalized gradient approximation made simple, *Phys. Rev. Lett.* 77 (1996) 3865–3868.
- [25] G. Kresse, D. Joubert, From ultrasoft pseudopotentials to the projector augmented-wave method, *Phys. Rev. B* 59 (1999) 1758–1775.
- [26] P.E. Blöchl, Projector augmented-wave method, *Phys. Rev. B* 50 (1994) 17953–17979.
- [27] Y. Li Huang, Y. Lu, T.C. Niu, H. Huang, S. Kera, N. Ueno, A.T.S. Wee, W. Chen, Reversible single-molecule switching in an ordered monolayer molecular dipole array, *Small* 8 (2012) 1423–1428.
- [28] J.L. Zhang, J.L. Xu, T.C. Niu, Y.H. Lu, L. Liu, W. Chen, Reversible switching of a single-dipole molecule imbedded in two-dimensional hydrogen-bonded binary molecular networks, *J. Phys. Chem. C* 118 (2014) 1712–1718.
- [29] H. Song, C. Fu, N. Li, H. Zhu, Z. Peng, W. Zhao, J. Dai, L. Xing, Z. Huang, W. Chen, Y. Wang, J. Yang, K. Wu, On the shuttling mechanism of a chlorine atom in a chloroaluminum phthalocyanine based molecular switch, *Phys. Chem. Chem. Phys.* 19 (2017) 22401–22405.
- [30] J.L. Zhang, J.Q. Zhong, J.D. Lin, W.P. Hu, K. Wu, G.Q. Xu, A.T.S. Wee, W. Chen, Towards single molecule switches, *Chem. Soc. Rev.* 44 (2015) 2998–3022.
- [31] C. Stadler, S. Hansen, I. Kröger, C. Kumpf, E. Umbach, Tuning intermolecular interaction in long-range-ordered submonolayer organic films, *Nat. Phys.* 5 (2009) 153–158.
- [32] T. Miller, W.E. McMahon, T.C. Chiang, Interference between bulk and surface photoemission transitions in Ag(111), *Phys. Rev. Lett.* 77 (1996) 1167–1170.
- [33] M.-K. Lin, Y. Nakayama, C.-Y. Wang, J.-C. Hsu, C.-H. Pan, S.-i. Machida, T.-W. Pi, H. Ishii, S.J. Tang, Interfacial properties at the organic-metal interface probed using quantum well states, *Phys. Rev. B* 86 (2012) 155453.
- [34] M.-K. Lin, Y. Nakayama, C.-H. Chen, C.-Y. Wang, H.T. Jeng, T.-W. Pi, H. Ishii, S.J. Tang, Tuning gap states at organic-metal interfaces via quantum size effects, *Nat. Commun.* 4 (2013) 2925.
- [35] T. Niu, M. Zhou, J. Zhang, Y. Feng, W. Chen, Dipole orientation dependent symmetry reduction of chloroaluminum phthalocyanine on Cu(111), *J. Phys. Chem. C* 117 (2013) 1013–1019.
- [36] S.-J. Tang, C.Y. Lee, C.C. Huang, T.R. Chang, C.M. Cheng, K.D. Tsuei, H.T. Jeng, V. Yeh, T.-C. Chiang, Electronic versus lattice match for metal-semiconductor epitaxial growth: Pb on Ge (111), *Phys. Rev. Lett.* 107 (2011) 066802.
- [37] M. Yakes, M.C. Tringides, Probing the buried Pb/Si(111) interface with SPA LEED and STM on Si(111)-Pb $\sqrt{3}\times\sqrt{3}$, *J. Phys. Chem. A* 115 (2011) 7096–7104.
- [38] S.-J. Tang, T. Miller, T.-C. Chiang, Modification of surface states in ultrathin films via hybridization with the substrate: a study of Ag on Ge, *Phys. Rev. Lett.* 96 (2006) 036802.